Lab on a Chip

Accepted Manuscript

ROYAL SOCIETY OF CHEMISTRY

www.rsc.org/loc

Formation of Elongated Fascicle-Inspired 3D Tissues Consisting of High-Density, Aligned Cells Using Sacrificial Outer Molding

By *Devin Neal*, *Mahmut Selman Sakar*, *Lee-Ling S. Ong*, *and H. Harry Asada**.

[*]Devin Neal, Prof. H. Harry Asada
Department of Mechanical Engineering
Massachusetts Institute of Technology
77 Massachusetts Avenue, Room 1-007, MA 02139 (USA)
E-mail: asada@mit.edu

Dr. Mahmut Selman Sakar
Institute of Robotics and Intelligent Systems
ETH Zurich
Zurich, CH 8092 (Switzerland)

Dr. Lee-Ling S. Ong
Singapore-MIT Alliance for Research and Technology (SMART) Center
1 CREATE Way
#04-13/14 Enterprise Wing, 138602 (Singapore)

Table of Contents Entry

Fascicle-inspired tissue strips are generated having high (~100s) length to diameter ratios using a novel external sacrificial molding method. High levels of alignment, 3D cell distribution, and cell density are demonstrated.

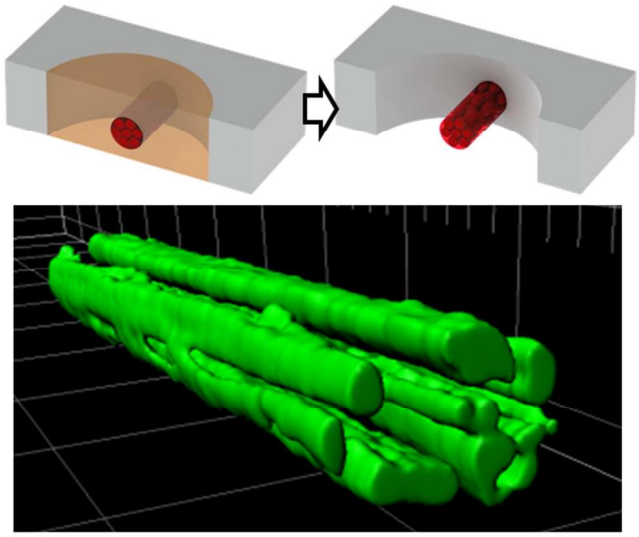

Abstract

The majority of muscles, nerves, and tendons are composed of fiber-like fascicle morphology. Each fascicle has a) elongated cells highly aligned with the length of the construct, b) a high volumetric cell density, and c) a high length-to-width ratio with a diameter small enough to facilitate perfusion. Fiber-like fascicles are important building blocks for forming those tissues of various sizes and cross-sectional shapes, yet no effective technology is currently available for producing long and thin fascicle-like constructs with aligned, high-density cells. Here we present a method for molding cell-laden hydrogels that generate cylindrical tissue structures that are ~100 μm in diameter with an extremely high length to diameter ratio (>100:1). Using this method we have successfully created skeletal muscle tissue with a high volumetric density (~50%) and perfect cell alignment along the axis. A new molding technique, Sacrificial Outer Molding, allows us to i) create a long and thin cylindrical cavity of desired size in a sacrificial mold that is solid at a low temperature, ii) release gelling agents from the sacrificial mold material after cell-laden hydrogel is injected into fiber cavities, iii) generate a uniform axial tension between anchor points at both ends that promotes cell alignment and maturation, and iv) perfuse the tissue effectively by exposing it to media after melting the sacrificial outer mold at 37°C. Effects of key parameters and conditions, including initial cavity diameter, axial tension, and concentrations of hydrogel and gelling agent, upon tissue compaction, volumetric cell density, and cell alignment are presented.

Introduction

There is a class of tissues that transmit forces, displacements, and even signals over significant distances. These tissues include muscles, tendons, and nerves. Cells within these tissues are significantly elongated along the axis of transmission, and tightly bundled with other

cells into fascicle structures [1, 2]. Multiple fascicles are bundled along with auxiliary cell types into the full tissue. Although the size and structure of the whole tissue varies greatly depending on specific location and function, all of these consist of fascicles that are largely the same in size and function. These tissues exhibit a hierarchical structure, where fascicles *in vivo* may be viewed as the structural unit at the highest hierarchical level, the assembly of which is the whole tissue. They act as functional building blocks to form tissue of diverse sizes and shapes. Fascicles have some morphological traits and features common to all of them: 1) their significant length is much larger than the width of an individual cell, 2) they are aligned along the axis of transmission, and 3) they have high volumetric density of cells to concentrate transmission. Furthermore, fascicles size is limited to a particular diameter so that centrally located cells may be perfused effectively [3]. The long and thin, cylindrical shape of the fascicle would facilitate to construct tissues with diverse cross-sectional shapes to meet the needs of specific tissue groups. Rather than directly building monolithic bulk tissue, the formation of building-block tissues inspired by fascicles that possess these features is an important step for constructing a full-scale tissue of this class. We present a method to produce fascicle-inspired tissues with tightly controlled parameters by generating a scaffold that is engineered to have 1) a truly 3D structure with controlled diameter and length, and 2) an aligned hydrogel nanostructure generated through anisotropic stress along the length of the construct.

Formation of fascicle-like tissues having all the three morphological features is a challenge. Prior works have successfully produced tissues focusing on one or two features. Photomasks [4], additive rapid prototyping [5], and gas foaming methods [6] have been used to create 3D tissue where highly aligned cell morphology is not required [7]. Various surface techniques have been utilized that pattern substrates with channels of diverse sizes [8, 33], or

chemical patterns, or even optical patterns for hydrogel polymerization on a surface. Such methods are designed to achieve highly aligned cell morphology and have successfully been employed to study fibroblast [8] and kidney epithelial cell orientation [9], muscle cell alignment [10, 34] and axon guidance [11]. Another substrate based technique to generate 3D tissue is to start with 2D cell sheets and either roll the cell sheets [10, 12] or stack them [32]. To generate 3D, aligned tissue scaffolds of biocompatible materials and hydrogels, electrospinning [13, 14], and microfluidic spinning [15, 16, 17] techniques have been used. Spun scaffold materials are typically composed of fibers with diameters larger than the cells seeded onto them. Therefore, the volumetric density of cells is inevitably low. Another method of generating highly aligned, 3D cell morphology is to seed cells in bulk hydrogel permanent molds and allow the initial cell mediated compaction to align the nanostructure of the hydrogel around controllable post/anchoring architectures [18, 19, 20]. This approach produces tissue constructs where cells tend to migrate towards the peripheral surface of the tissue, leaving a low density of cells inside. The average cell density across the full tissue cross section is therefore low for larger diameter constructs. The micro-post technology has successfully produced aligned 3D skeletal muscle tissues [20, 21]. While the compliance of the posts facilitates to measure force and displacement, it allows the tissue to relax, reducing stress in the tissue.

Despite these advances, to our knowledge, no technology is currently available that successfully produces fascicle-like 3D constructs, grown in a 3D scaffold environment, having a high aspect ratio on the order of 100:1, and a high volumetric density of highly aligned cells. In this work, we present a method of producing cell-seeded hydrogel strips with controllable properties that produce aligned 3D fascicle-like tissue constructs with a high cell density and a high aspect ratio utilizing a novel multiple molding method.

Results and Discussion

Sacrificial External Molding

Multiple molding steps were utilized in the fabrication of the device. An initial shallow aluminum mold with steel pins spanning the width of the aluminum mold was used to cast PDMS slabs with numerous properly sized and spaced through holes (Fig. 1A and B). Once removed from the aluminum mold (Fig. 1C), the PDMS slabs were cut into multiple PDMS chips, each with a single through hole (Fig. 1D). 5 mm well holes were punched in a line ~ 3 mm apart along the through hole of each chip. These PDMS chips were then bonded to glass forming 3 wells per device (Fig. 1E). In each device, a steel pin was inserted on each side of the through hole such that each pin spanned one of the two outer 5 mm wells to be used as seeding wells. The central well was to be used as a media reservoir.

To produce an elongated, highly dense fascicle structure in a robust and consistent manner, we form the fascicle hydrogel within a soft sacrificial mold that constrains the hydrogel to generate a desired cylindrical shape. Fig. 2A shows a permanent PDMS mold with a horizontal through hole. A removable spacer pin, made of a simple cylindrical steel pin, is inserted into the through hole (Fig. 2Ai). Warm liquid sacrificial mold material, such as gelatin, is filled into the permanent mold with the spacer pin in place. A key aspect of this method is that reagents to facilitate the gelling of the scaffold hydrogel are dissolved in the sacrificial mold material. Once cooled solid (typically at 4° C), the spacer pin is removed by hand from the sacrificial mold leaving a cavity tube (Fig. 2Aii), and cells mixed with a dissolved hydrogel precursor are seeded into the cavity tube (Fig. 2Aiii). The device is then warmed to a temperature where the sacrificial mold melts. As the sacrificial mold material liquidizes, the dissolved gelling reagents freely diffuse into the scaffold hydrogel (Fig. 2Aiv). The scaffold hydrogel solidifies

due to the combined effects of temperature and gelling reagents. Lastly, 37° C media is infused via an adjacent media reservoir well adjacent to the seeding well to remove the melted sacrificial mold material (Fig. 2Av). The entire fascicle-like construct is fully exposed to the surrounding media, facilitating perfusion throughout the experiment.

The novelty in this method is that the outer sacrificial mold becomes liquid as the inner hydrogel becomes solid. This process is diagramed in detail in Fig. 2B. At a low temperature (such as 4º C) the sacrificial mold is solid and the inner cell/hydrogel solution is liquid. As the device is warmed to 37 ºC, the sacrificial mold melts releasing a gelling agent. At 37 ºC, the inner hydrogel has become solid, and the sacrificial mold has become completely liquid. The inner hydrogel is then freely suspended across the seeding well, anchored to the PDMS walls.

Our method of creating suspended hydrogel strips exploits the properties that 1) the melting temperature of a sacrificial mold material overlaps with the temperature range of the hydrogel gelation and 2) hydrogel crosslinking agents embedded in the sacrificial mold material are released into the hydrogel as the melting/gelation occurs. See Fig. 2B. These phenomena allowed us to mold the hydrogel within a sacrificial mold and then simultaneously melt the sacrificial mold and crosslink the hydrogel. This strategy prevents the hydrogel solution from solidifying during the injection process, which occurs if the hydrogel is mixed with crosslinking agents before injection. Furthermore, no hard substrate or solid surface is used for forming the hydrogel. This eliminates any difficulty in removing the hydrogel from a permanent mold without sticking, facilitating highly uniform, consistent, and reliable production of very high aspect ratio constructs.

The use of sacrificial molds has been reported in prior cell culture works, however, only as a removal layer [22] or as internal molds (positive molds) [23, 24, 25] rather than outer molds

(negative molds). For example, microvascular-like channels have been produced in a Collagen I gel by using a removable or sacrificial material as an internal mold. Once the internal mold is removed, a scaffold with embedded microchannels is created, and endothelial cells were seeded into the scaffold. We present a contrasting method as we invert the "inside" and "outside" materials. By exchanging the removable and permanent materials, we produce a device (Fig. 2) with the unique features described above. The resultant fascicle-like construct is not in contact with any hard substrate, yet a desired shape is created. To our knowledge there is no prior work on using 1) a sacrificial material, like gelatin, as an outer sacrificial mold for cell seeded hydrogels, or on utilizing 2) the overlapping external melting/internal gelation temperatures of the materials used.

In order for this method to work, the sacrificial mold material must be solid at the temperature at which the hydrogel solution is injected. If the sacrificial mold material is not solid, no cavity will be formed in which to inject the hydrogel solution. The sacrificial mold material must be liquid at a temperature below a level affecting cell viability, ideally below 37 ºC. See Fig.2B. For practical implementation purposes, the ideal temperature for injection is room temperature (20 ºC), and the material should have a viscosity low enough to inject into the seeding wells around the spacer pins without introducing inconsistencies and/or bubbles into the seeding wells. We have found that gelatin dissolved in culture media at a concentration of 5-20% satisfies these requirements (See supplementary information for more details).

Using fibrin as an exemplary hydrogel, we demonstrate that we can release a gelling agent (thrombin) from the sacrificial mold material. Fibrin is produced through interaction of two materials. Fibrinogen is the primary precursor component of fibrin, mixed with seeding cells. Thrombin is a serine protease that converts fibrinogen into gel-forming fibrin strands [26].

Thrombin is dissolved in the sacrificial mold material and reacts with fibrinogen when the sacrificial mold melts. Additionally, fibrin has been shown to be a good scaffold for producing aligned contractile skeletal muscle cells [19, 27].

An alternative to dissolving thrombin in the sacrificial mold material is to mix the thrombin and fibrinogen solution immediately before injecting. There are significant drawbacks to using this alternative method because of the quick onset of gelation once thrombin is mixed with fibrinogen. The viscosity of the cell laden hydrogel keeps changing as the property of fibrinogen changes during injection, leading to a non-homogeneous fibrin strip. If multiple devices are being seeded at once, it is particularly difficult to inject uniformly into multiple devices to create multiple fascicle strips because of the added time. These non-uniformities may also generate randomly distributed stress concentrations affecting cell behavior. Conversely, dissolving thrombin in the sacrificial mold allows us to fully control the gelation timing; gelation does not occur until the temperature is increased to approximately 37 ºC. (See supplementary information for more details).

We began preliminary work using this method to embed multiple cell types including motor neurons in embryoid bodies, fibroblasts, tenocytes, and skeletal myoblasts in multiple hydrogels including fibrin, and PEG hydrogels (See Supplementary Fig. S1). Here, we focus on results from seeding C2C12 mouse myoblasts in fibrin hydrogels.

Fascicle-like tissue formation

Fig. 3A shows a developed fascicle-like tissue 14 days after seeding with C2C12 formed myotubes distributed throughout the length of the tissue. The total length of the tissue is 5 mm, while the diameter is ~100 μm, resulting in an aspect ratio of 50:1. This tissue is the result of

using a single steel spacer pin in a single seeding well. Striations of α-actinin along the length of each myotube are clearly visible (Fig. 3C) indicating multiple myotubes in a single construct have sarcomeric structure capable of contraction (Supplemental Movie 1). Phase contrast images (Fig. 3D) show that cells become more aligned, as the tissue develops from 2 to 14 days post seeding. By day 14, these tissues contain a high volumetric density of packed contractile muscle cells aligned axially along the full length of the fascicle. The cross section images in Fig. 3B demonstrate that myotubes are densely populated throughout the tissue. Two distinct features of the method were exploited to produce these fascicle-like constructs with dense, aligned cells; 1) controlled scaffold geometry ensures that diffusion-based transport is possible for internally located cells, and 2) cells align passively along the axis of the scaffold material due to cell mediated compaction of the hydrogel.

In the above experiments we have observed the fascicle-like construct becomes taut, indicating that internal tension is generated between the two ends. The whole construct is not constrained by any substrate except for both ends where the hydrogel adheres to the permanent mold. Therefore, the tension is uniform throughout the construct along the longitudinal axis. This internal stress acts to align the fibrils of the hydrogel that provide alignment cues to the seeded cells [28, 29]. It is important to generate uniform tension throughout gel development to align the hydrogel fibrils uniformly. This is a passive process requiring no external effort to induce such aligning stress.

Importance of axial stress

To investigate the role of the stress generated between two anchored ends of the hydrogel, and its effects on cell density and alignment, we conducted a series of experiments. In one experiment, we relieved the generated stress by disconnecting one end of each taut construct from the permanent mold two days after seeding as diagramed in Fig. 3G. The resulting constructs all compacted significantly towards the remaining anchored end (Fig. 3I). This resulted in two significant differences from control constructs; 1) the cell density was lower, and 2) there were fewer, and less mature myotubes. The cross section of these constructs reveals that cells occupy only the periphery of the compacted construct and that the volumetric cell density is low (Fig. 3J). This is consistent with previous results reported for larger diameter constructs, where there is a central void of active cells when the diameter is large enough to inhibit diffusion based processes [19]. Secondly, within the peripheral space were cells existed in the single anchored constructs, α-actinin, a contractile protein, was found in only a few short, unaligned myotubes (Fig. 3I). In contrast, constructs maintained in suspension between two anchors produced significantly more and more mature myotubes that were longer and aligned with the axis of the tissue (Fig. 3A). This is consistent with previously reported results showing the value of stress induced alignment on the fusion and differentiation of myoblasts [20]. This shows that even in the surface regions where diffusion is not limited, myoblast differentiation does not ready occur without stress. These two effects combine to result in significantly lower amounts of α-actinin (Fig. 3H). In another experiment, we examined the potential aligning effects due to cell fusion (myotube formation). We prohibited myoblasts from differentiating to fused myotubes by increasing ε-aminocaproic acid concentration to 10 mg ml^{-1} in the media [30], and examined whether the individual cells still align or not. Fig. 3E and F show that, although the cells were arrested in the myoblast phase, the cells densely populated the interior of the constructs and were

aligned with their nuclei elongated along the longitudinal axis. Therefore, the cells align without fusion under stress.

Construct diameter

To examine the effect of scaffold geometry, constructs made with various removable spacer pin diameters were produced, and changes in construct diameters were monitored via phase contrast images over the course of two weeks as the myoblasts developed into functional myotubes (Fig. 4A). The diameter varies along the length of tissue construct. We measured the diameter at each point along the length and at each time point by using custom MATLAB code. Fig. 4B shows changes to the average diameter computed for the entire length of each construct over 10 days.

In each construct, significant compaction occurred within the first day. This is consistent with prior works on initial cell mediated compaction of cell laden fibrin [18, 29, 31]. After the first day, the diameter of the developing constructs slowly decreased continuously. The ratio of the cross sectional area at a particular time point to the initial cross sectional area (A_t/A_0) of a construct (the 'area ratio'), was independent of initial diameter for the first few days (Fig. 4C). We observed that the initial gel compaction is fairly independent of the gel's geometric size. However, as time progressed, constructs with smaller diameters had substantially smaller area ratios, compared to those of larger diameter constructs. This indicates that over time, smaller diameter constructs remodel the fibrin scaffold to a greater degree resulting in greater compaction than the larger diameter constructs. In other words, the longer-term interactions between cells and their surrounding scaffold material are more active for the thinner constructs,

where the cells are perfused properly. Increasing construct diameter limits diffusion based processes of internally located cells.

We normalize the variations in construct diameter by dividing the standard deviation of the construct diameter with its mean value. Fig. 4D shows this normalized standard deviation for constructs with different initial diameters. Over time, the standard deviation tends to increase, indicating that the initial construct geometry is more uniform. Of significance is the result that smaller diameter constructs tend to increase in variation, (i.e. decrease in uniformity), more so than larger diameter constructs. Therefore, in designing tissue construct by choosing the initial spacer pin diameter, there is a trade-off between volumetric density of contractile cells (Fig. 4C) and uniformity of the cross section (Fig. 4D) along the construct.

Cell density

To quantify the volumetric cell density, α-actinin, a marker of mature myotubes, was imaged via confocal microscopy, and its total volume was determined. The volumetric density of α-actinin was calculated as the ratio of the total volume of α-actinin to the total volume of the construct (Fig. 5C). Total volume is approximated from final diameter data generated from phase contrast images using custom MATLAB code (Fig. 5A), while α-actinin volume (Fig. 5B) is calculated from 3D reconstruction via Imaris software generated from confocal image stacks (Fig. 5D). The ratio of α-actinin volume to total volume (Fig. 5C) serves as a measure of developed myotube density within the construct that can objectively be used to compare constructs grown under different conditions.

The presented method has produced a high cell density of over 50% in terms of α-actinin volume ratio, as shown in Fig. 5C. It allows us to vary several key parameters that affect the

fascicle formation. These parameters include initial diameter, fibrinogen concentration within the injected hydrogel-cell suspension, and thrombin concentration dissolved in the sacrificial mold. As expected, both the total volume and α-actinin volume are positively correlated with initial diameter size (Fig. 5A,B). Interestingly though, the volumetric density of α-actinin is higher for constructs with smaller initial diameters; over 50% volumetric density was achieved for the diameter of 254μm (Fig. 5C). Smaller initial diameter constructs end up with higher concentrations of contractile cells, leading us to hypothesize that increasing construct diameter limits diffusion based processes of internally located cells.

Fibrin component variation

When initial fibrinogen concentration was varied, constructs with higher fibrinogen concentration decreased in volume significantly more (Fig 5A). Despite this, there was no statistically significant variation in α-actinin volume for various concentrations of fibrinogen (Fig 5B). Combining these two results, the volumetric density of α-actinin is greater for higher concentrations of fibrinogen than for lower concentrations (Fig. 5C).

Varying thrombin concentration produced similar results to varying fibrinogen concentration; the total resulting volume of the constructs was negatively correlated with thrombin concentration (Fig. 5A), while the volume of α-actinin was uncorrelated to thrombin concentration (Fig. 5B). The resulting volume ratio of α-actinin was thus positively correlated with thrombin concentration (Fig. 5C). We hypothesis that these results occur because increased thrombin concentration results in a greater density of cross linking of the fibrin gel and this may lead to cells exerting greater compaction forces if the cell density is maintained high enough.

These results demonstrate that the these three groups of molding parameters, a) sacrificial mold geometry, e.g. diameter, b) hydrogel concentration, and c) crosslinking agent concentration, can be used to vary and tune key properties of fascicle-like constructs, such as cell density and construct size, in a statistically significant manner.

Conclusions

In summary, the sacrificial outer molding method allows us to produce fascicle-like 3D constructs consisting of densely populated (over 50% volumetric cell density), aligned cells with a high aspect ratio (~100:1). This was made possible by exploiting three major features of the method: 1). The outer mold is sacrificial, and releases hydrogel crosslinking agents when melting, resulting in a scaffold simply suspended between two anchoring ends, with no solid substrate; 2). Cell-mediated compaction of the hydrogel creates uniform internal tensile force along the length of the construct, which aligns the cells and promotes maturation; and 3) The sacrificial outer mold with a tunable diameter provides the hydrogel with an initial geometric constraint and allows the 3D construct to be exposed to a surrounding media, facilitating perfusion across the entire cross section of the construct. The present molding method is flexible and expandable to a broad class of cell types, providing a unique approach to formation of fascicle-like constructs.

Materials and Methods

Fabrication of Permanent Molds: The aluminum mold, shown schematically in Fig. 1A, was milled using a 3/16" end mill for the pocket and a #77 or larger drill bit for the holes in the sides of the pocket. The default pin diameter was nominally 356 μm. When pin diameter was treated as the independent variable, pin diameters of 254, 305, 356, 508, 787 and 1016 μm were used (McMaster-Carr). The aluminum and a single pack of steel pins cost less than $25.

Culture of C2C12 Myoblasts: C2C12 mouse myoblasts (Ameican Type Culture Collection) were cultured in growth medium (GM) containing DMEM (American Type Culture Collection), supplemented with 10% fetal bovine serum (FBS, Sigma-Aldrich), 1% penicillin-streptomycin 100X (Invitrogen), and 0.1 mg ml^{-1} Normacin (Invivogen). Confluence was kept below 70%.

Casting of Sacrificial Mold and Hydrogel Constructs: The 3 wells of each device were rinsed with PBS (Invitrogen) and aspirated. Gelatin (Sigma-Aldrich) was added to GM at a concentration of 5% w/v and melted at 37° C. 1% 0.5 M NaOH and thrombin were added to the gelatin solution which was then immediately injected into the seeding wells of the devices, submerging the steel spacer pin spanning the each seeding well. The devices were then cooled at 4° C for 20 minutes to solidify the gelatin. The default concentration for thrombin was 1 U ml^{-1}. Thrombin concentrations of 0, 0.1 U ml^{-1}, 1 U ml^{-1}, and 10 U ml^{-1} were used when thrombin concentration was treated as the independent variable.

The cell/hydrogel mixture was prepared by mixing fibrinogen (Sigma-Aldrich), Matrigel (BD Biosciences) (20% v/v), and C2C12 myoblasts (10E6 cells ml^{-1}) with GM and kept on ice. The default concentration of fibrinogen was 5 mg ml^{-1}. When fibrinogen was treated as the independent variable, its concentration varied between 1.25, 2.5, 5, and 10 mg ml^{-1}.

The devices were seeded by removing the steel spacer pin spacers from the solid gelatin sacrificial mold, and injecting the cell/hydrogel mixture, via micropipette, into the cavity formed by the spacer pins. Immediately after seeding, the devices are placed into an incubator at 37° C and 5% CO2. After 30 to 60 minutes, GM is added to the medium reservoir well. GM in the media reservoir is replaced daily twice, then replaced with differentiation medium (DM) comprised of DMEM, 10% horse serum (Sigma-Aldrich), 1% penicillin-streptomycin 100X, and 0.1 mg ml^{-1} Normacin. Experiments were terminated 14 days after initial seeding.

Immunostaining: Samples were fixed with 4% paraformaldehyde at room temperature for 15 minutes, rinsed with PBS, permeabilized with 0.5% Triton-X (Sigma-Aldrich) in PBS for 20 minutes, and blocked with a mixture of 10% goat serum (Sigma-Aldrich) v/v, 1% w/v bovine serum albumin (Sigma-Aldrich) in PBS for 1 hour all at room temperature. Samples were treated with the primary antibody for sarcomeric α-actinin (Invitrogen) at a 200:1 dilution for 1 hour at room temperature, followed by the Alexa Fluor 488 secondary antibody (Invitrogen) at a dilution of 200:1 overnight at 4° C.

Automated Image Analysis: Custom scripts written in MATLAB (Mathworks), determined the changes in diameter along the muscle strips. To determine the strip from the background, the differences in image intensity in the x and y directions at each pixel in the image were combined. Larger pixel intensities correspond to the muscle strip. Otsu thresholding was applied to segment the strip in the image [32]. We determined the first and last thresholded pixel along the x direction of the image to be its top and bottom edges. A straight line was fitted on centerline pixels. The angle of the strip to the horizontal (x-axis) was calculated from the slope of this

line. The top and bottom pixel coordinates were rotated at this angle so that the strip was horizontally aligned. The diameter at each x-coordinate was calculated as the difference between the top and bottom y-coordinates.

Acknowledgements

This material is based on work supported in part by the National Science Foundation, under Grant No. CBET-0939511, the Science and Technology Center for Emergent Behaviors of Integrated Cellular Systems (EBICS), and in part by the Singapore-MIT Alliance of Research and Technology, BioSyM IRG.

References

[1] P. L. Williams, Gray's Anatomy, New York: Churchill Livingstone, 1995.

[2] R. L. Lieber, Skeletal muscle structure, function and plasticity: the physiological basis of rehabilitation, Lippincott Williams & Wilkins, 2002.

[3] A. C. Paul, "Muscle length affects the architecture and pattern of innervation differently in leg muscles of mouse, guinea pig, and rabbit compared to those of human and monkey muscles," *The Anatomical Record,* vol. 262, no. 3, pp. 301-309, 2001.

[4] V. L. Tsang, A. A. Chen, L. M. Cho, K. D. Jadin, R. L. Sah, S. DeLong, J. L. West and S. N. Bhatia, "Fabrication of 3D hepatic tissues by additive photopatterning of cellular hydrogels," *The FASEB Journal,* vol. 21, no. 3, pp. 790-801, 2007.

[5] V. Chan, P. Zorlutuna, J. H. Jeong, H. Kong and R. Bashir, "Three-dimensional

photopatterning of hydrogels using stereolithography for long-term cell encapsulation," *Lab on a Chip,* vol. 10, no. 16, pp. 2062-2070, 2010.

[6] S. Partap, I. Rehman, J. R. Jones and J. A. Darr, "“Supercritical Carbon Dioxide in Water” Emulsion-Templated Synthesis of Porous Calcium Alginate Hydrogels," *Advanced Materials,* vol. 18, no. 4, pp. 501-504, 2006.

[7] P. Zorlutuna, N. Annabi, G. Camci-Unal, M. Nikkhah, J. M. Cha, J. W. Nichol, A. Manbachi, H. Bae, S. Chen and A. Khademhosseini, "Microfabricated biomaterials for engineering 3D tissues," *Advanced Materials,* vol. 24, no. 14, pp. 1782-1804, 2012.

[8] J. Yang, F. R. Rose, N. Gadegaard and M. R. Alexander, "A High-Throughput Assay of Cell-Surface Interactions using Topographical and Chemical Gradients," *Advanced Materials,* vol. 21, no. 3, pp. 300-304, 2009.

[9] K. M. Schumacher, S. C. Phua and J. Y. Ying, "Controlled formation of biological tubule systems in extracellular matrix gels in vitro," *Kidney international,* vol. 73, no. 10, pp. 1187-1192, 2008.

[10] M. T. Lam, S. Sim, X. Zhu and S. Takayama, "The effect of continuous wavy micropatterns on silicone substrates on the alignment of skeletal muscle myoblasts and myotubes," *Biomaterials,* vol. 27, no. 24, pp. 4340-4347, 2006.

[11] K. J. Jang, M. S. Kim, D. Feltrin, N. L. Jeon, K.-Y. Suh and O. Pertz, "Two distinct filopodia populations at the growth cone allow to sense nanotopographical extracellular matrix cues to guide neurite outgrowth," *PLoS One,* vol. 5, no. 12, p. e15966, 2010.

[12] R. G. Dennis, P. E. Kosnik, M. E. Gilbert and J. A. Faulkner, "Excitability and contractility of skeletal muscle engineered from primary cultures and cell lines," *Am J Physiol Cell*

Physiol, vol. 280, no. 2, pp. C288-C295, 2001.

[13] S. Y. Chew, R. Mi, A. Hoke and K. W. Leong, "The effect of the alignment of electrospun fibrous scaffolds on Schwann cell maturation," *Biomaterials,* vol. 29, no. 6, pp. 653-661, 2008.

[14] H. B. Wang, M. E. Mullins, J. M. Cregg, A. Hurtado, M. Oudega, M. T. and Trombley and R. J. Gilbert, "Creation of highly aligned electrospun poly-L-lactic acid fibers for nerve regeneration applications," *Journal of neural engineering,* vol. 6, no. 1, p. 016001, 2009.

[15] C. M. Hwang, Y. Park, J. Y. Park, K. Lee, K. Sun, A. Khademhosseini and S. H. Lee, "Controlled cellular orientation on PLGA microfibers with defined diameters," *Biomedical microdevices,* vol. 11, no. 4, pp. 739-746, 2009.

[16] E. Kang, Y. Y. Choi, S. K. Chae, J. H. Moon, J. Y. Chang and S. H. Lee, "Microfluidic Spinning of Flat Alginate Fibers with Grooves for Cell-Aligning Scaffolds," *Advanced Materials,* vol. 24, no. 31, pp. 4271-4277, 2012.

[17] H. Onoe, T. Okitsu, A. Itou, M. Kato-Negishi, R. Gojo, D. Kiriya, K. Sato, S. Miura, S. Iwanaga, K. Kuribayashi-Shigetomi, Y. T. Matsunaga, Y. Shimoyama and S. Takeuchi, "Metre-long cell-laden microfibres exhibit tissue morphologies and functions," *Nature Materials,* vol. 12, no. 6, pp. 584-590, 2013.

[18] W. Bian and N. Bursac, "Engineered skeletal muscle tissue networks with controllable architecture," *Biomaterials,* vol. 30, no. 7, pp. 1401-1412, 2009.

[19] S. Hinds, W. Bian, R. G. Dennis and N. Bursac, "The role of extracellular matrix composition in structure and function of bioengineered skeletal muscle," *Biomaterials,* vol. 32, no. 14, pp. 3575-3583, 2011.

[20] H. Vandenburgh, J. Shansky, F. Benesch-Lee, V. Barbata, J. Reid, L. Thorrez, R. Valentini and G. Crawford, "Drug-screening platform based on the contractility of tissue-engineered muscle," *Muscle and nerve,* vol. 37, no. 4, pp. 438-447, 2008.

[21] M. S. Sakar, D. Neal, T. Boudou, M. A. Borochin, Y. Li, R. Weiss, R. D. Kamm, C. S. Chen and H. H. Asada, "Formation and optogenetic control of engineered 3D skeletal muscle bioactuators," *Lab on a Chip,* vol. 12, no. 23, pp. 4976-4985, 2012.

[22] M. Muraoka, T. Shimizu, K. d Itoga, H. Takahashi and T. Okano, "Control of the formation of vascular networks in 3D tissue engineered constructs," *Biomaterials,* vol. 34, no. 3, pp. 696-703, 2010.

[23] K. R. King, C. C. J. Wang, M. R. Kaazempur-Mofrad, J. P. Vacanti and J. T. Borenstein, "Biodegradable microfluidics," *Advanced Materials,* vol. 16, no. 22, pp. 2007-2012, 2004.

[24] A. P. Golden and J. Tien, "Fabrication of microfluidic hydrogels using molded gelatin as a sacrificial element," *Lab on a Chip,* vol. 7, no. 6, pp. 720-725, 2007.

[25] L. M. Bellan, M. Pearsall, D. M. Cropek and R. Langer, "A 3D Interconnected Microchannel Network Formed in Gelatin by Sacrificial Shellac Microfibers," *Advanced Materials,* vol. 24, no. 38, pp. 5187-5191, 2012.

[26] J. W. Weisel, "Fibrinogen and fibrin," *Adv. Protein Chem.,* vol. 70, pp. 247-299, 2005.

[27] Y. C. Huang, R. G. Dennis, L. Larkin and K. Baar, "Rapid formation of functional muscle in vitro using fibrin gels," *Journal of Applied Physiology,* vol. 98, no. 2, pp. 706-713, 2005.

[28] A. E. X. Brown, R. I. Litvinov, D. E. Discher, P. K. Purohit and J. W. Weisel, "Multiscale mechanics of fibrin polymer: gel stretching with protein unfolding and loss of water," *Science,* vol. 325, no. 5941, pp. 741-744, 2009.

[29] E. A. Sander, V. H. Barocas and R. T. Tranquillo, "Initial fiber alignment pattern alters extracellular matrix synthesis in fibroblast-populated fibrin gel cruciforms and correlates with predicted tension," *Annals of biomedical engineering,* vol. 39, no. 2, pp. 714-729, 2011.

[30] À. Díaz-Ramos, A. Roig-Borrellas, A. García-Melero, A. Llorens and R. López-Alemany, "Requirement of Plasminogen Binding to Its Cell-Surface Receptor α-Enolase for Efficient Regeneration of Normal and Dystrophic Skeletal Muscle.," *PLos ONE,* vol. 7, no. 12, 2012.

[31] E. Kim, O. V. Kim, K. R. Machlus, X. Liu, T. Kupaev, J. Lioi, A. S. Wolberg, D. Z. Chen, E. D. Rosen, Z. Xu and M. Alber, "Correlation between fibrin network structure and mechanical properties: an experimental and computational analysis," *Soft Matter,* vol. 7, no. 10, pp. 4983-4992, 2011.

[32] H. Takahashi, T. Shimizu, M. Nakayama, M. Yamato, T. Okano, "The use of anisotropic cell sheets to control orientation during the self-organization of 3D muscle tissue," *Biomaterials,* vol. 34, pp. 7372-7380, 2013.

[33] K. S. Suh, Y. S. Kim, H. H. Lee, "Capillary Force Lithography," *Advanced Materials ,* vol. 13, pp. 1386-1389, 2001.

[34] H. S. Yang, N. Ieronimakis, J. H. Tsui, H. N. Kim, K-Y Suh, M. Reyes, D-H Kim, "Nanopatterned muscle cell patches for enhanced myogenesis and dystrophin expression in a mouse model of muscular dystrophy," *Biomaterials ,* vol. 35, pp. 1478-1486, 2014.

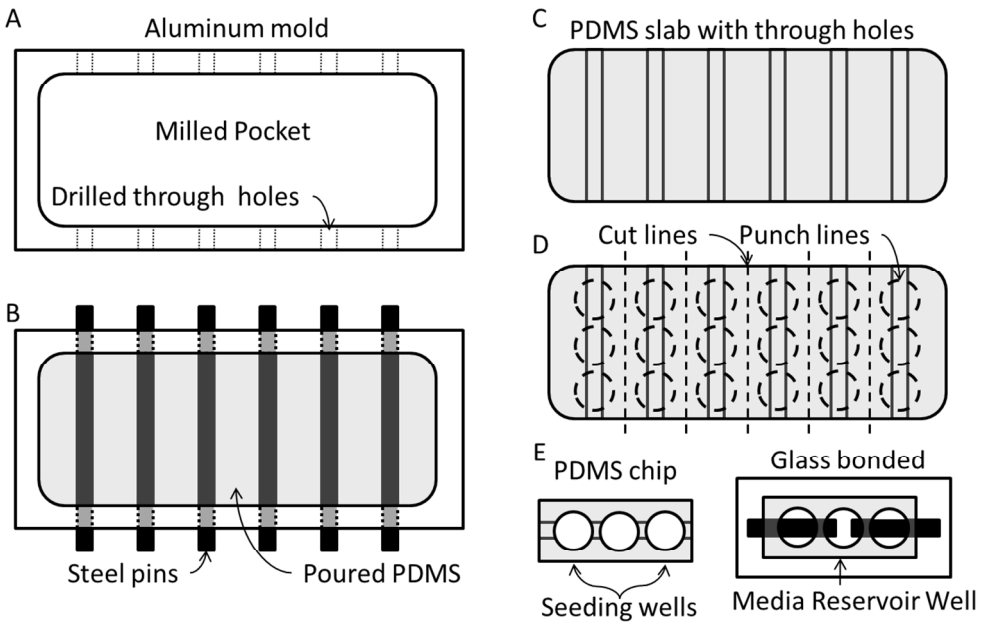

Figure 1. Schematic of production of PDMS permanent molds. A) A machined aluminum mold consisting of an aluminum bar with a milled pocket and several drilled through holes. B) multiple steel pins spanning the milled pocket with PDMS poured over, filling the pocket. C) A PDMS slab after removal of the steel pins, and the slab from the milled pocket. D) Cut and punch lines showing how the slab is made into individual chips. E) an individual PDMS chip, and a final device consisting of a PDMS chip bound to glass with steel pins inserted into the seeding wells.

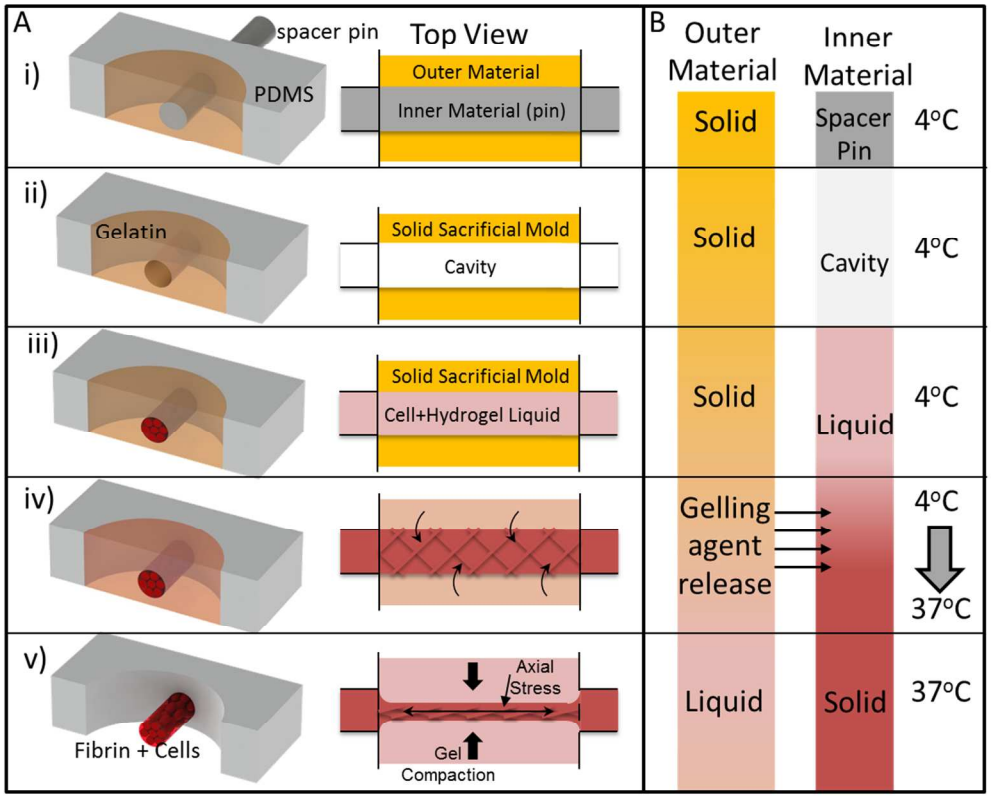

Figure 2. Fascicle-like tissue construct production technique utilizing a sacrificial outer mold, the overlap of mold melting temperature/hydrogel gelling temperature, and cell mediated compaction. (A) Schematic cross sectional and top view of multi-molding stage technique. (B) Upon heating to 37° C, the gelatin melts and the hydrogel begins to solidify as gelling agents dissolved in the gelatin are released into hydrogel upon melting of the gelatin, then cell mediated gel compaction generates anisotropic stress.

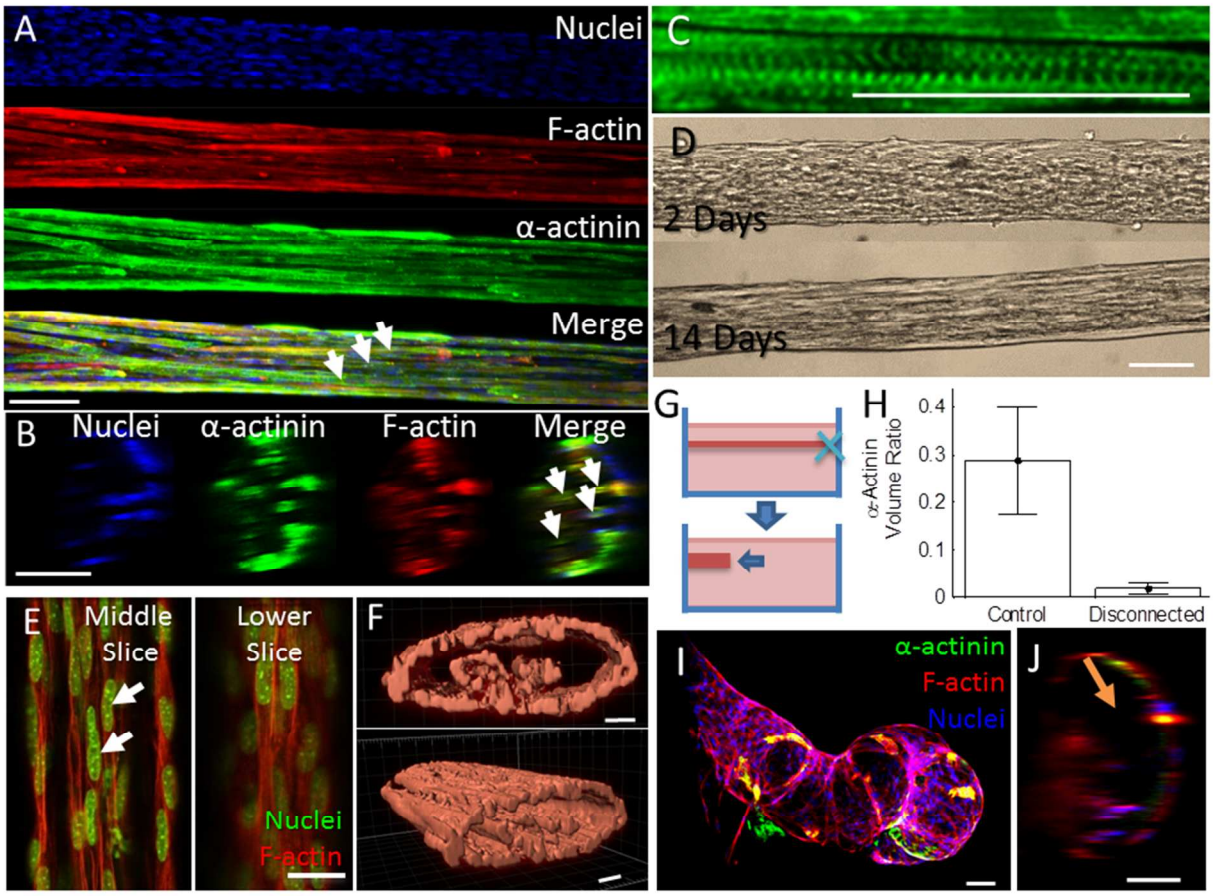

Figure 3. Longitudinal stack (A), and axial slice (B) confocal images of developed fascicle-like structure of C2C12 myotubes showing high volumetric density of aligned cells (white arrows) and contractile protein, α-actinin. (C) Clear striations of α-actinin within myotubes. (D) Phase contrast images of a cell seeded construct showing progressive alignment of cells from 2 days to 14 days. (E) 2-Photon microscope images of a construct with C2C12 cells arrested in the myoblast state showing alignment of actin and elongated nuclei (white arrows) and (F) Imaris renderings of F-actin showing cell populated internal regions without myotube formation. (G) Schematic sideview of a seeding well with a construct with one end disconnected from the wall 2 days after seeding. (H) Volumetric density of sarcomeric protein, α-actinin, with both ends anchored (control) vs. single-anchor-removed (disconnected) constructs (n=5). Longitudinal stack (I) and axial section (J) confocal images of fascicle like constructs having had one end disconnected 2 days after seeding showing poor volumetric density, poor myotube formation and a large central region void of cell (orange arrow). Scale bars 50 μm for A-E,I,J and 10 μm for F.

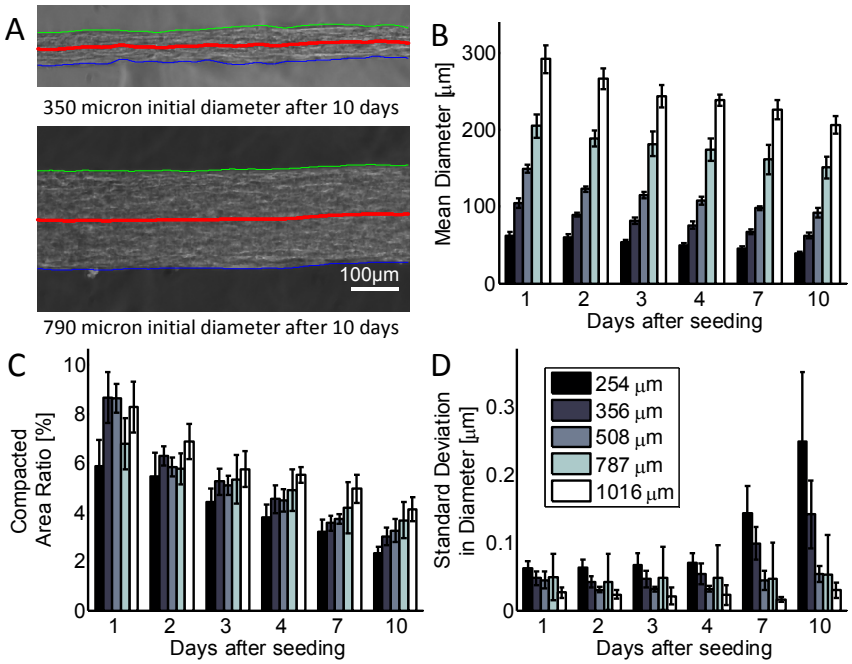

Figure 4. Geometric changes in fascicle construct structure over time. (A) Phase contrast images analyzed with custom MATLAB code to measure diameter at each point along the construct. The green, red, and blue lines indicate the top, center, and bottom of the tissue. (B) Mean diameters of individual constructs with differing initial diameters decrease gradually over time. (C) The compacted area ratio (the ratio of the mean compacted cross sectional area to its initial cross sectional area) shows little initial dependence on diameter 1 day after seeding, and decreases over time. After 10 days, the compacted area ratio is dependent on initial diameter. (D) The standard deviation of diameter along single constructs for various initial diameters is independent of initial diameter after 1 day, and increases over time, but increases faster for constructs with smaller initial diameters.

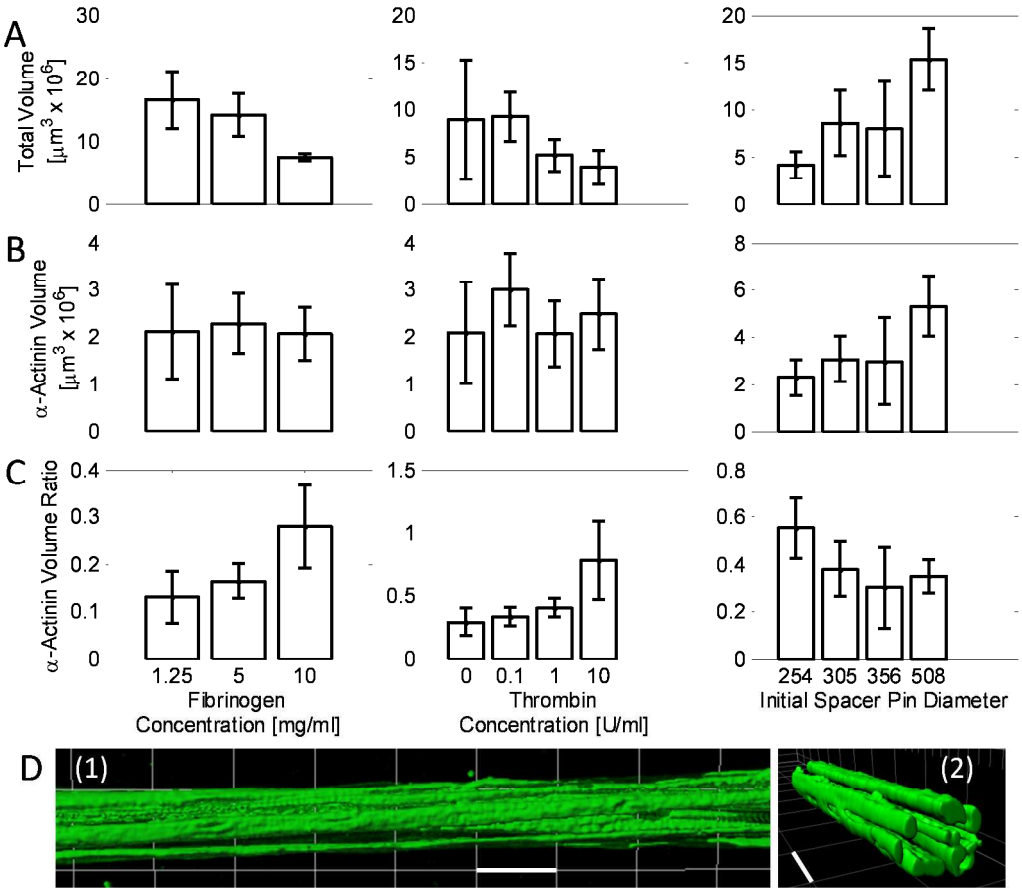

Figure 5. Variable parameters may be used to control the development of fascicle-like constructs. Total volume (A), volume of contractile protein α-actinin (B), and volumetric density of contractile protein α-actinin after 14 days of development (C) in relation to initial fibrinogen density, thrombin concentration, and initial diameter (n=5-6). Increasing concentration of fibrinogen and thrombin decreases total volume (A) while leaving α-actinin volume unchanged (B), resulting in high α-actinin density for higher concentrations of fibrinogen and thrombin (C). Increasing initial diameter increases both total volume (A) and α-actinin volume (B) but decreases α-actinin density (C). (D) A top view (1) and perspective view (2) of the volumetric density of α-actinin in a single typical construct. Scale bars 50 μm.